BIU Journal of Basic and Applied Sciences 9(1): 97 – 114, 2024.

ISSN: 2563-6424

CHARACTERISATION OF SUBSURFACE MATERIALS USING GEOELECTRICAL IMAGING IN OWANOBA, EDO STATE, NIGERIA

***AVENBUAN, N. AND IDUSERI, O. M.**
Department of Physical Sciences, Faculty of Science, Benson Idahosa University, Benin City, Nigeria
*Corresponding author: navenbuan@biu.edu.ng

ABSTRACT

This paper presents data from exploration of Subsurface Stratification in Owanoba Community, Ikpoba-Okha Local Government Area, Edo State, Nigeria, using Geophysical Methods. The survey area spans longitudes 005° 40′ 12.0″ E to 005° 40′ 19.0″ E and latitudes 06° 07′ 11.1″ N to 06° 07′18.3″ N within Owanoba. The study engaged 2D imaging to investigate the subsurface stratification in both the vertical and horizontal spreads at the Owanoba community. The electrical resistivity data obtained in parallel and orthogonal equidistant lines were processed into geoelectric models using RES2DINV. The survey data were collated and inverted as a single 3D data set using RES3DINV software and Voxler 4.0 to produce 3D depth slices and a 3D block model for subsurface stratification. The study of the 2D pseudo-section showed four geoelectric layers in the OWANOBA area, which are indicative of topsoil, dry laterite, dry lateritic soil, and sandstones. The resistivity lithology in the study areas revealed the presence of four geoelectric layers extending to a significant depth of 40 meters: topsoil (807 – 1462 Ωm), dry laterite (1462 – 4793 Ωm), dry lateritic soil (1462 – 2647 Ωm), and sandstones (925 – 1462 Ωm). The lithology corroborates the borehole logs within the environs. The presence of distinct resistivity layers suggests varying geological formations, likely influencing groundwater flow and construction considerations. Topsoil and dry lateritic layers indicate potential for agricultural use but also susceptibility to erosion. Dry laterite suggests weathered iron-rich material, while sandstones may signify a stable aquifer. The consistency with borehole logs enhances confidence in the interpretation. Overall, the findings suggest a heterogeneous subsurface with implications for land use planning, hydrogeological assessments, and infrastructure development.

KEYWORDS: *Sandstones, subsurface stratification, dry laterite, electrical resistivity, Owanoba*

INTRODUCTION

Soil, referred to as a substance, comprises rock particles transformed through chemical and mechanical processes, such as weathering and associated erosion mechanisms. It develops a porous structure and can be conceptualized as a three-state system, involving solids (minerals like clay, silt, and sand), liquids (water), and gases (air) (Rhodes, 2012). The depth of the horizons can vary considerably from one to another, and the boundaries between them are rarely sharply defined. Since the pore

space of soil contains both gases and water, the aeration of the soil influences not only the health of the flora and fauna but also the emission of greenhouse gases (Rhodes, 2012).

Analysing soil stratification can be helpful in so many research areas, such as agriculture, road construction, botany, building foundations, groundwater assessment and monitoring, pollution of contaminants, and so on. There are several ways of stratifying the soil. Coring is the best approach, but one of the most efficient and effective approaches is geophysical means, which is a non-invasive method of determining the subsoil strata (Avenbuan *et al.*, 2020a). Of all the geophysical approaches, electrical resistivity has the most widespread application in resolving geophysical problems, including groundwater, contaminant plumes, road construction, etc. (Avenbuan *et al.*, 2020b; Reynolds, 2011; Loke *et al*., 2013; Telford *et al.*, 1990).

A two-layer model, such as depth to bedrock, is commonly a benchmark product that will motivate data compilation and clarify priorities for data collection, such as geophysics and drilling. A point file of bedrock surface elevations may undergo machine modelling by some method deemed appropriate after iterative approaches or may be modelled by hand and digitised to introduce expert opinion on the most likely rock surface geometry. Many regional jurisdictions and nations now have maps for depth to bedrock or depth to the basement for large areas exceeding 100,000 km^2 (Gao *et al*., 2006).

In this investigation, an extensive examination of subsurface materials within the Owonoba region of Edo State, Nigeria was undertaken. Situated in the southern part of Nigeria, Owonoba boasts a rich variety of geological formations, rendering it an optimal site for studying subsurface materials (Iduseri and Alile, 2021). The present study to employed geoelectrical imaging technique to map and characterize diverse subsurface strata, encompassing topsoil, lateritic soil, sandstone, and lateritic subsoil. Through the analysis of resistivity fluctuations at various depths and lateral distances. The study aims to obtain a deeper understanding of the geological composition prevalent in the study area. The outcomes of this research are anticipated to furnish valuable insights for land-use planning and the advancement of infrastructure within Owonoba and analogous geological environments.

Geology of the Survey Area

Edo State is situated in the south-western part of Nigeria. It is an important sedimentary basin in Nigeria due to its closeness to the oil fields within the Niger Delta. The survey area, Owanoba (marked using a circle in Figure 1) is located in Ikpoba Okha Local Government Area of Edo State. The area occupies the southern part of Edo State, a sedimentary terrain, and is underlain by sedimentary rocks of Paleocene to recent age (Avenbuan *et al.*, 2020b). The sedimentary rock contains about 90% sandstone and laterites (Alile *et al*., 2011). The survey location lies within longitudes 005° 40' 12.0" E to 005° 40' 19.2" E and latitudes 06° 07' 11.2" N to 06° 07'18.7" N. It has a minimum elevation of 25 m and a maximum elevation of 52.3 m.

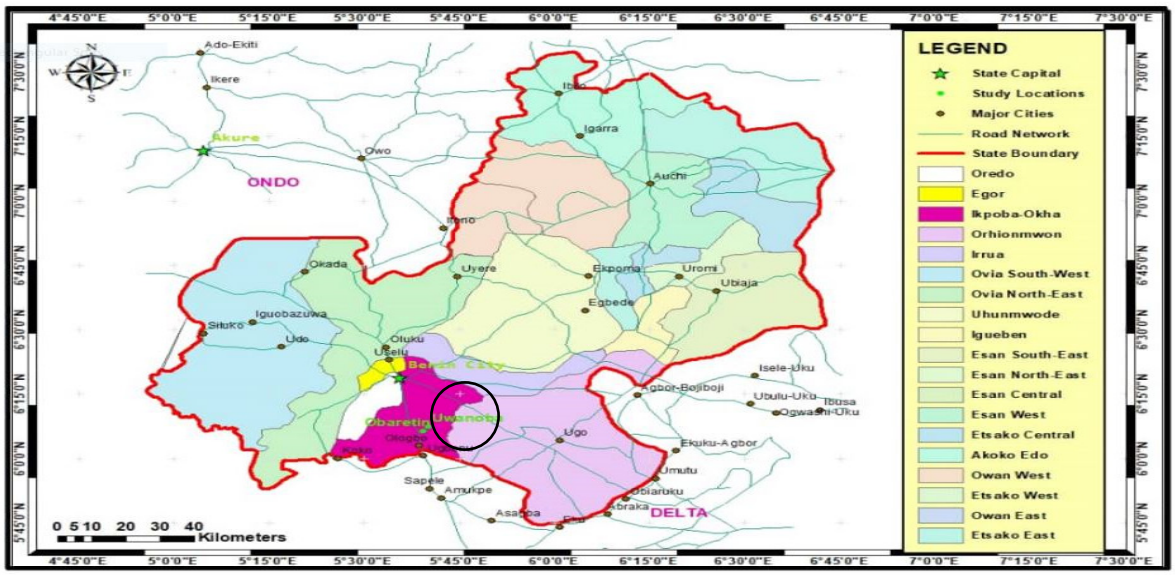

Fig. 1: The map of Edo State showing the location of the study area

METHODOLOGY

Field Theory

The Wenner array configuration technique (Figure 2) was deployed in the data collection. The choice of the configuration is largely because the arrays have moderate depths of investigation and generally strong signal strength, which is inversely proportional to the geometric factor used in calculating the apparent resistivity values. It is also preferred for surveys at noisy sites because of its high signal strength. In this configuration, electric current is introduced into the subsurface using a pair of current electrodes (C_1 and C2). This current creates an electric field within the subsurface. The electric potential distribution due to this injected current is measured across a pair of potential electrodes, P_1 and P_2. The resistance offered by the subsurface geologic feature is obtained by calculation using Ohm's law:

$$R = \frac{\Delta V}{I} \qquad \text{i}$$

Where:

ΔV is the electric potential difference across the potential electrodes; P_1 and P_2,

I is the current introduced into the subsurface using a pair of current electrode; C_1 and C_2.

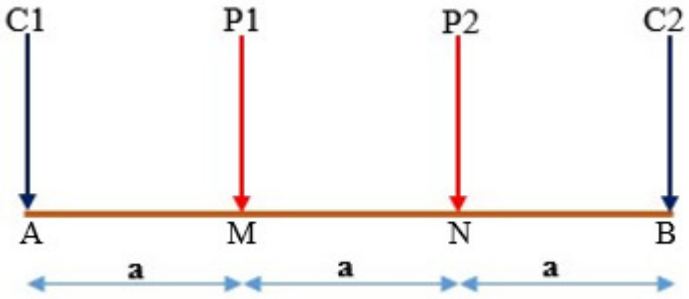

Fig. 2: Electrode configuration adopted for the survey

The potentials, V_M and V_N measured at the electrodes P_1 and P_2 respectively are

$$V_M = \frac{\rho I}{2\pi}\left[\frac{1}{AM} - \frac{1}{MB}\right] \; and \; V_N = \frac{\rho I}{2\pi}\left[\frac{1}{AN} - \frac{1}{NB}\right] \qquad \text{ii}$$

Where:
r is the resistivity of the medium
AM = NB = a; MB = AN = 2a
AM is the distance between electrodes C1 and P1
NB is the distance between electrodes P2 and C2
MB is the distance between electrodes P1 and C2
And AN is the distance between electrodes C1 and P2
The potential difference, ($\Delta V_{MN} = V_M - V_N$), between the two potential electrodes is given as

$$\Delta V_{MN} = V_M - V_N = \frac{\rho I}{2\pi}\left\{\left[\frac{1}{a} - \frac{1}{2a}\right] - \left[\frac{1}{2a} - \frac{1}{a}\right]\right\} = \frac{\rho I}{2\pi}\left\{\frac{1}{a} - \frac{1}{2a} + \frac{1}{a} - \frac{1}{2a}\right\}$$

$$= \frac{\rho I}{2\pi a} \qquad \text{iii}$$

The resistivity, ρ, is obtained by rearranging Equation iii, and is given as

$$\rho = \frac{2\pi a \Delta V_{MN}}{I} \qquad \text{iv}$$

$$\rho = KR \qquad \text{v}$$

$$Where \; K = 2\pi a \; and \; R = \frac{\Delta V_{MN}}{I}$$

K is called the geometric factor.

Data Acquisition

A total of five (5) 2D traverses were established along the parallel and orthogonal directions, as shown in Figure 3, in a grid format using the Wenner array configuration technique (Loke *et al.*, 2013). This electrode configuration was well suited for constant separation data acquisition systems so that many data points can be recorded simultaneously for each current injection. Measurements were made at sequences of electrodes at 10, 20, 30, 40, 50, and 60 m intervals using four (4) electrodes spaced 10 m apart with an inter-traverse spacing of 50 m from each other and a maximum length of 200 m each.

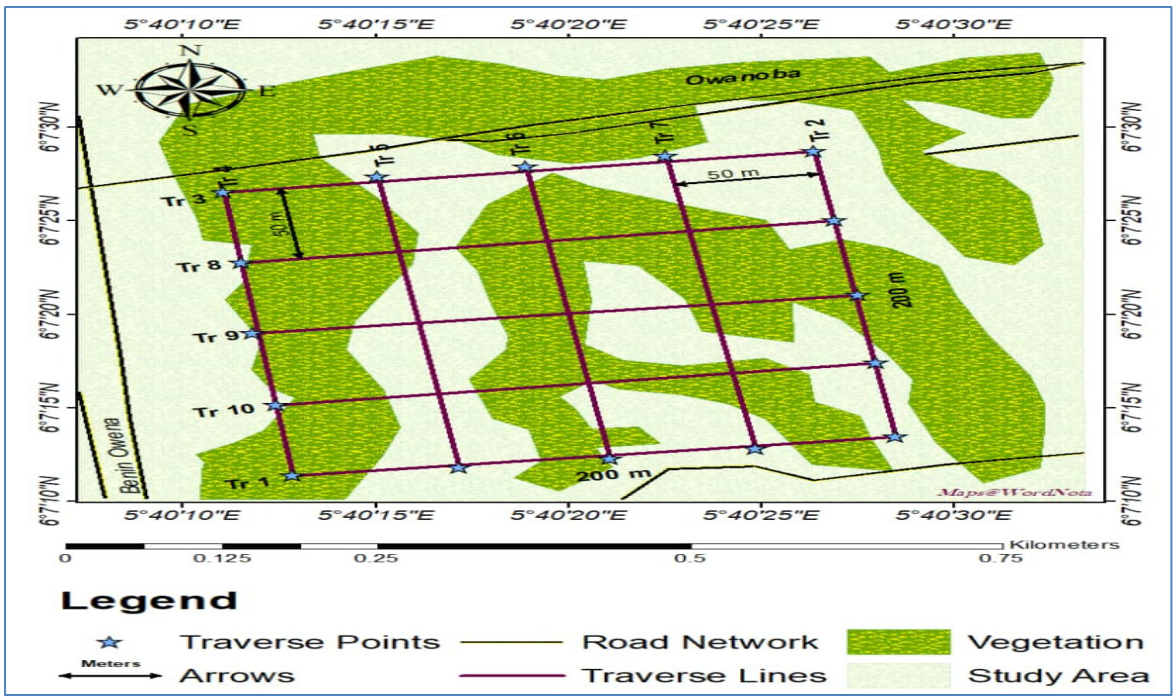

Fig. 3: Data acquisition map showing traverse lines in Owanoba

Data Processing/Interpretation

The RES2DINV software was used for the inversion of the 2D apparent resistivity data (Griffith *et al.*, 1993). After filtering out noise by exterminating bad data points, an inversion was done on the field data to produce the 2D resistivity models of the subsurface lithology. The RES2DINV programme amortises the bulk data into a series of horizontal and vertical rectangular blocks, with each box containing a number of records to reduce the RMS error. The resistivity of each block was then calculated to produce an apparent resistivity pseudo-section. The pseudo-section was compared to the actual measurements for a good model fit. The difference between measured and observed gives the inverse resistivity model, which represents the geology of the study area (Loke *et al.*, 1996).

The RES3DINV and the Voxler 4.0 software were used for the inversion of the 3D apparent resistivity data. The 2D data sets in RES2DINV format were collated into a single 3D data set using a batch file and consequently developed to obtain depth slices for each section and the 3D block model for the study area. The workflow is summarised as follows:

1. Combining a two-dimensional data set into a single three-dimensional data set
2. Inversion of the two-dimensional and three-dimensional data sets
3. Develop a three-dimensional block model of the three-dimensional inversion.

RESULT AND DISCUSSION

A lateral distance of 200 m was covered, and a maximum depth of 39.6 m was imaged across each of the ten traverses in Owanoba.

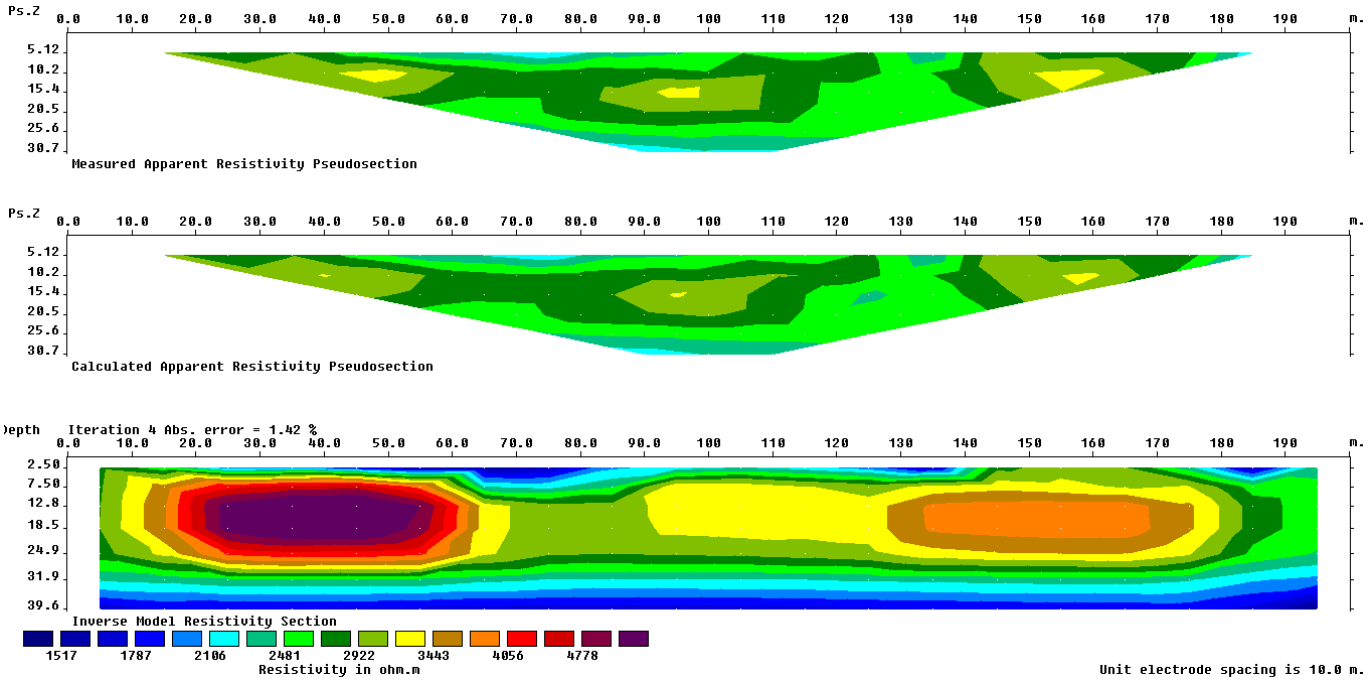

Fig. 4: 2D electrical resistivity pseudo-section along Profile 1 at Owanoba

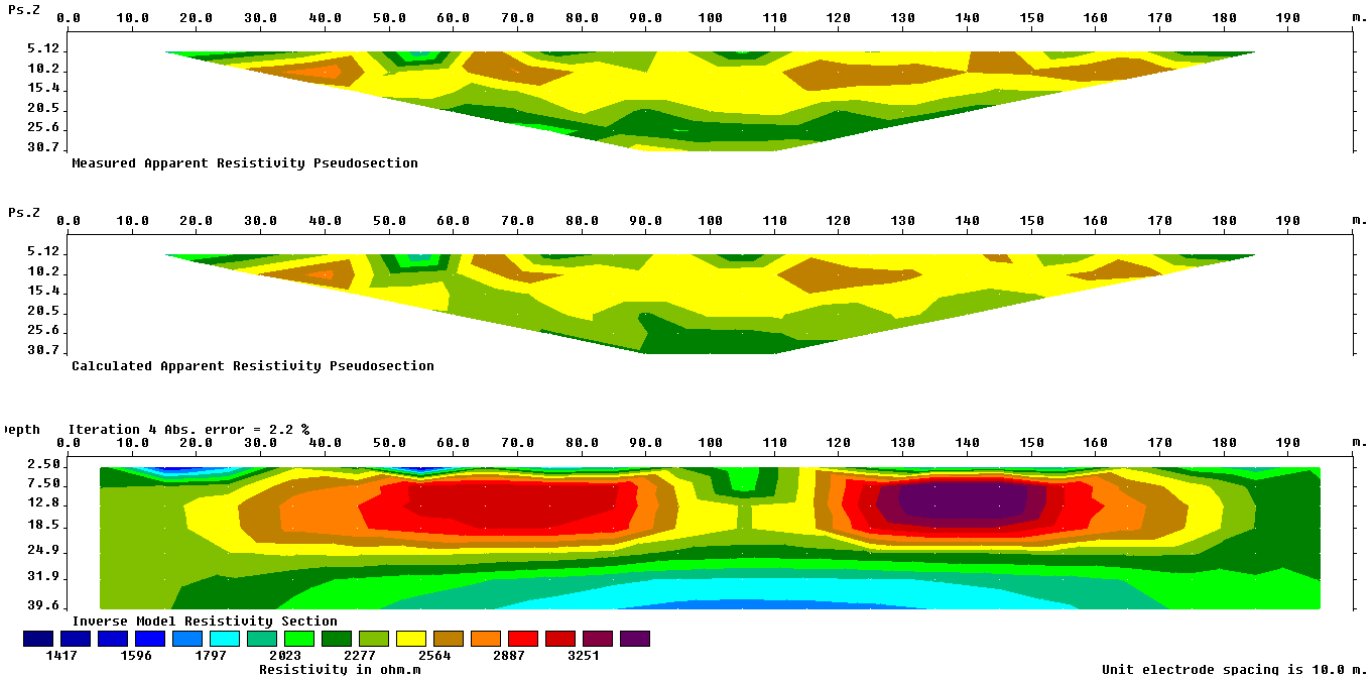

Fig. 5: 2D electrical resistivity pseudo-section along Profile 2 at Owanoba

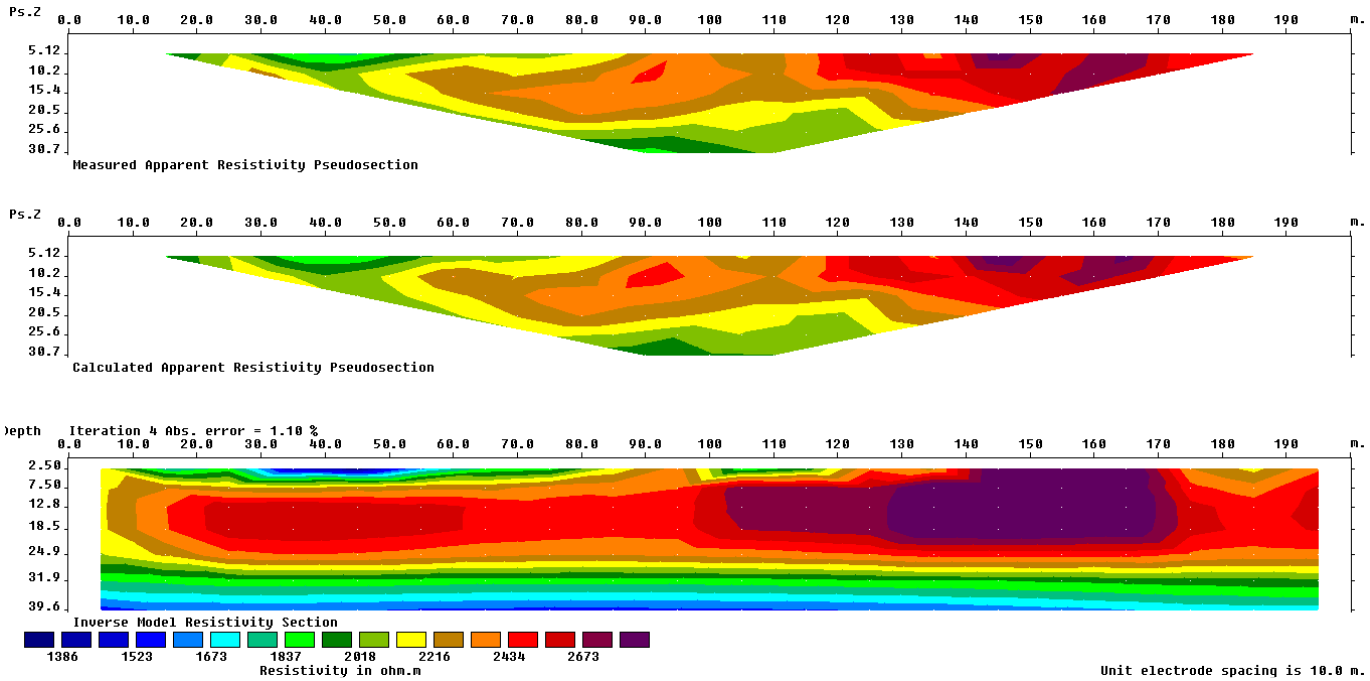

Fig. 6: 2D electrical resistivity pseudo-section along Profile 3 at Owanoba

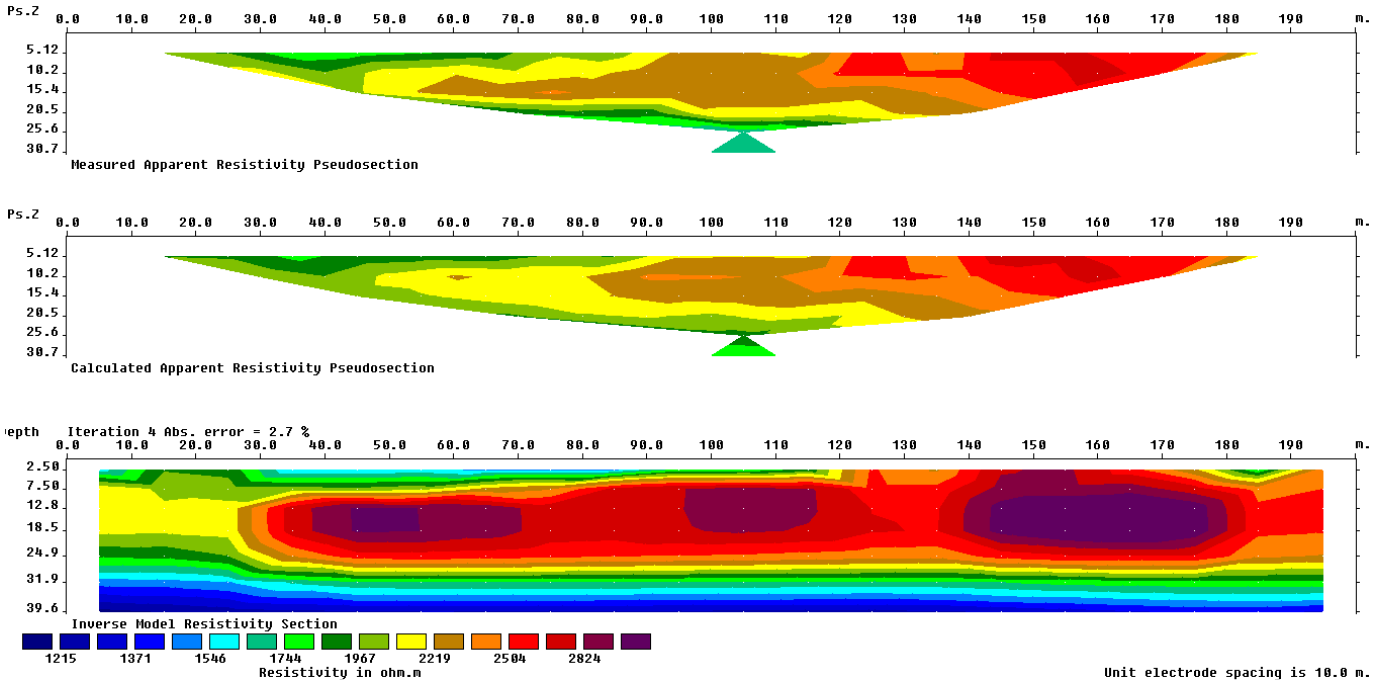

Fig. 7: 2D electrical resistivity pseudo-section along Profile 4 at Owanoba

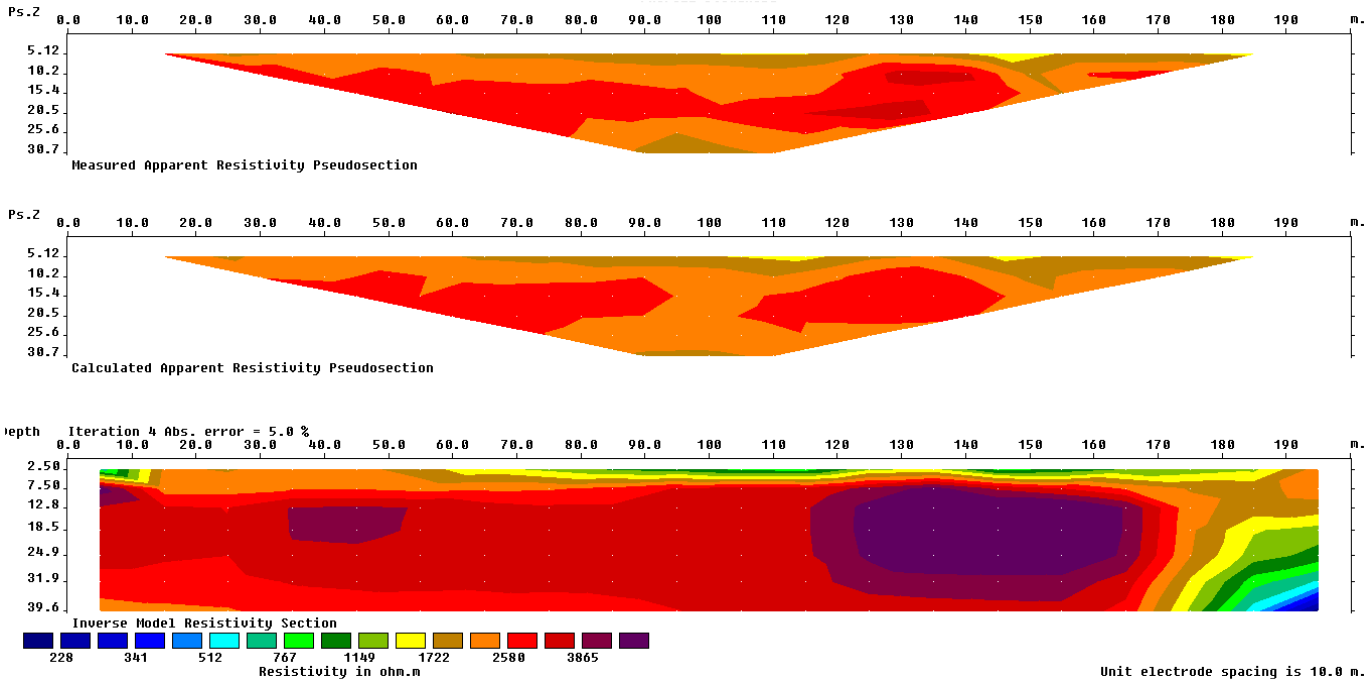

Fig. 8: 2D electrical resistivity pseudo-section along Profile 5 at Owanoba

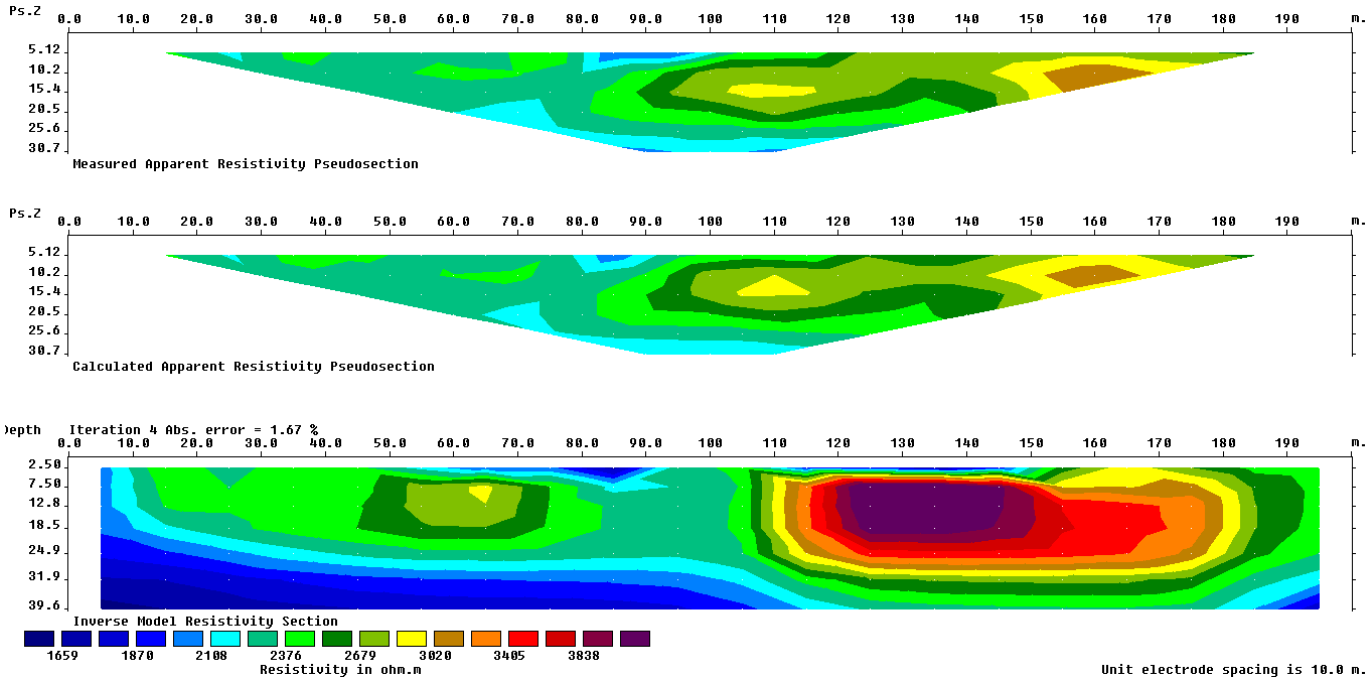

Fig. 9: 2D electrical resistivity pseudo-section along Profile 6 at Owanoba

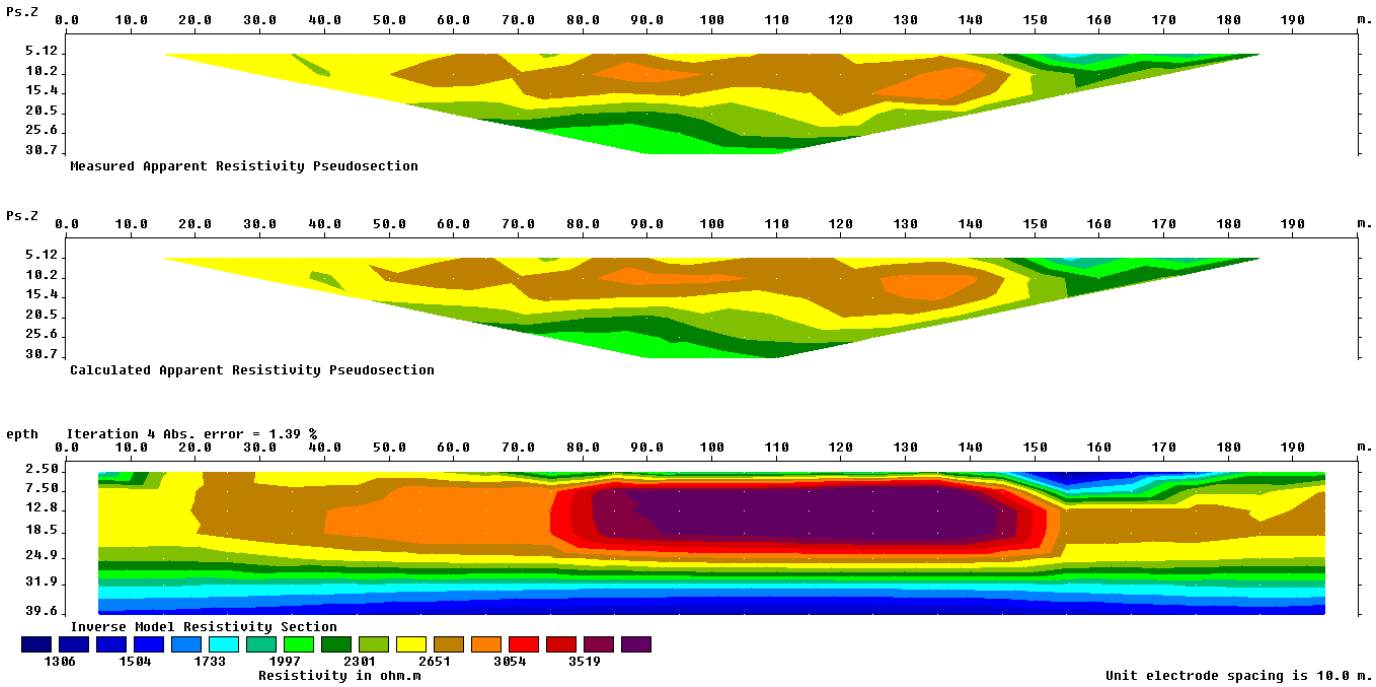

Fig. 10: 2D electrical resistivity pseudo-section along Profile 7 at Owanoba

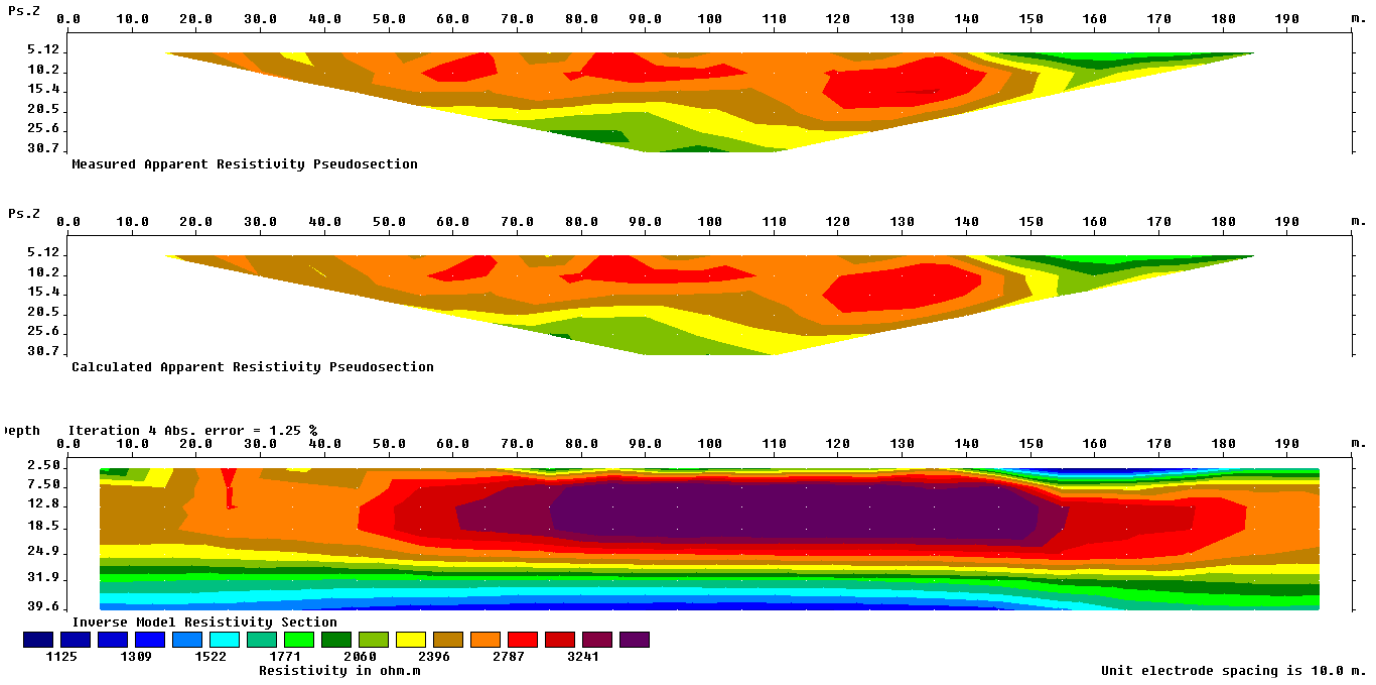

Fig. 11: 2D electrical resistivity pseudo-section along Profile 8 at Owanoba

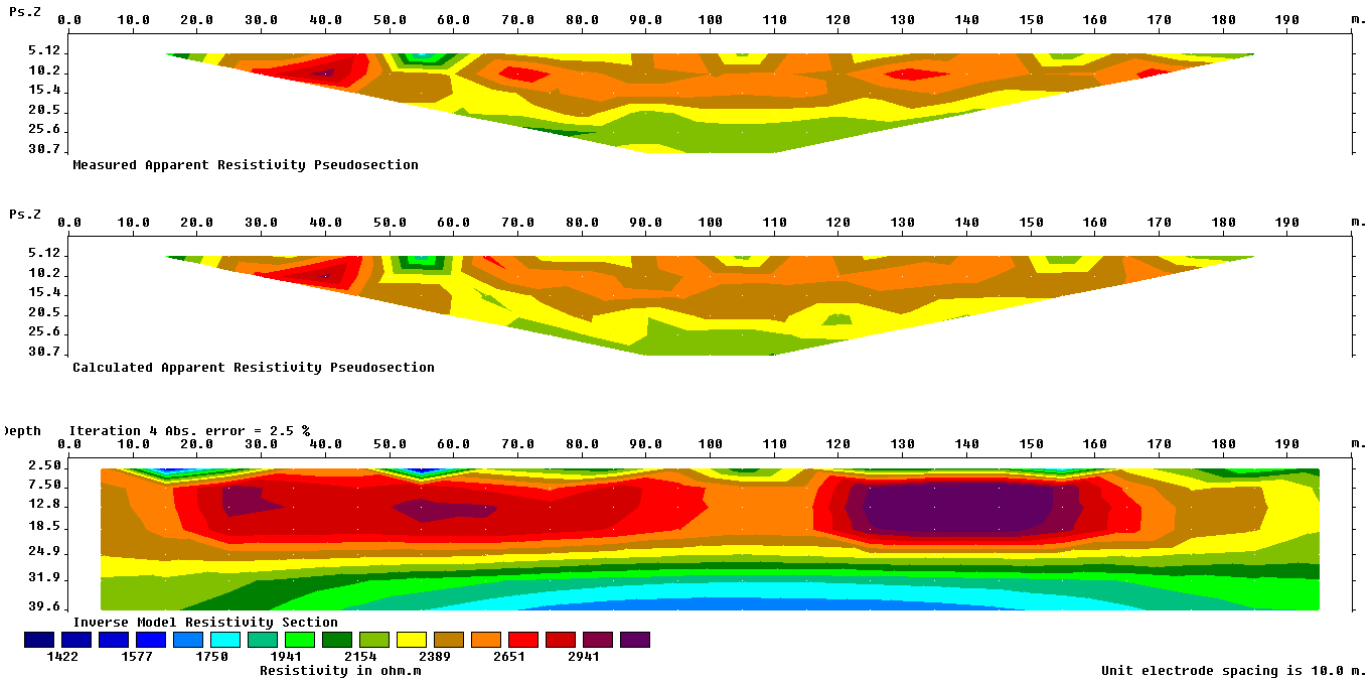

Fig. 12: 2D electrical resistivity pseudo-section along Profile 9 at Owanoba

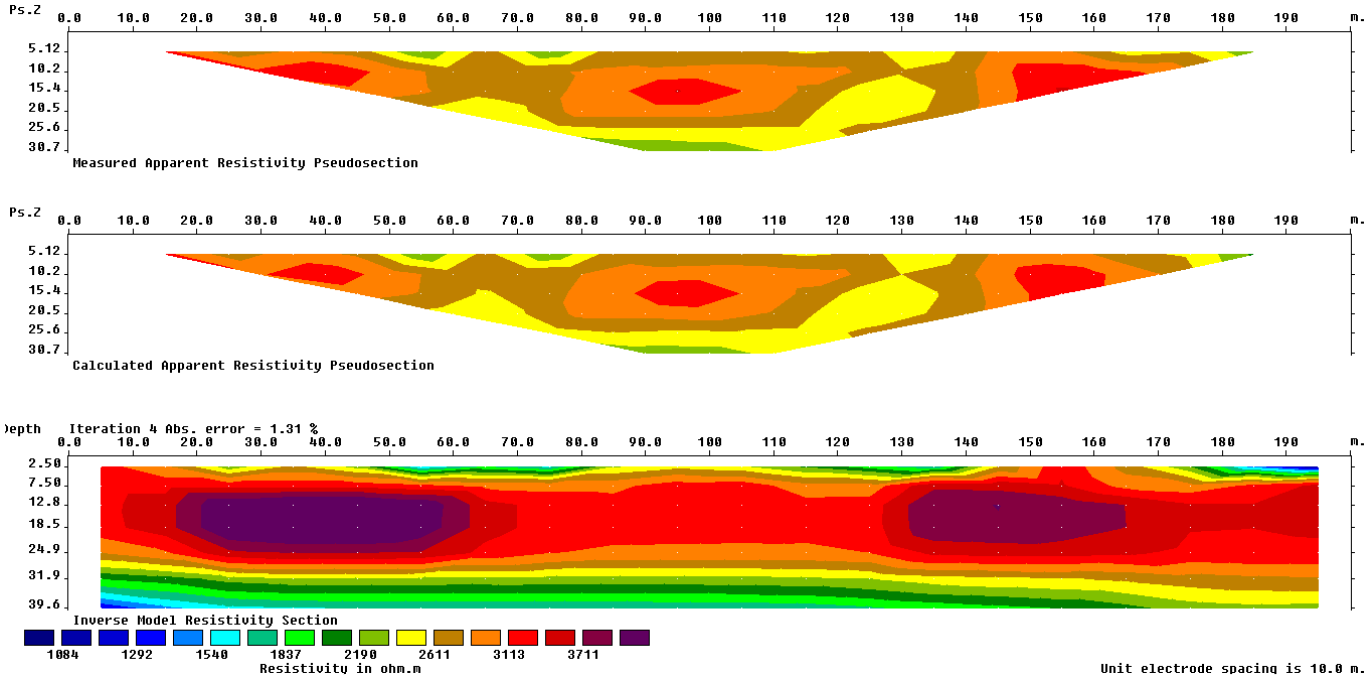

Fig. 13: 2D electrical resistivity pseudo-section along Profile 10 at Owanoba

In the depth range of 2.5 – 7.5 m, the resistivity image delineates topsoil with values ranging from 1554 – 5377 Ωm, spanning a lateral distance of 5 – 195 m (Fig. 4). At 7.5 – 24.9 m depth and a lateral distance of 20 – 55 m, the resistivity falls between 3777 and 5386 Ωm, indicative of dry laterite. Another substratum with

resistivity values of 1856 to 3741 Ωm occurs at 2.5 – 20 m depth, covering a lateral distance of 80 – 190 m, suspected to be sandstones. At 31.9 – 39.6 m depth and a lateral spread of 70 – 190 m, resistivity ranges from 1554 to 2217 Ωm, suggesting a lateritic subsoil.

The first geoelectric layer, as depicted in Fig. 5, comprises lateritic topsoil with sandstone intercalations, extending 2.5 meters thick from depths of 2.5 to 5 meters beneath the surface. Within this layer, resistivity values vary from 1596 to 2564 Ωm, with lateral distances spanning 5 to 195 meters. The subsequent subsoil layer, presumed to consist of sandstones, is encountered between depths of 5 and 24.9 meters, exhibiting resistivity values ranging from 2023 to 3251 Ωm. Beyond this depth, resistivity diminishes to a range of 1797 – 2277 Ωm, with the lowest values observed at lateral distances of 60 – 175 meters, indicative of lateritic subsoil.

The first layer, lateritic topsoil with sandstone intercalations, as depicted in Fig. 6, is 2.5 m thick from 2.5 to 5 m depth, exhibiting resistivity values ranging from 1523 to 2673 Ωm and extending laterally from 5 to 195 m. At a depth of 5 – 25 m, the second layer, presumed to consist of sandstones, presents resistivity values ranging from 2434 to 2673 Ωm. Beyond 25 m depth, resistivity values shift to the range of 1523 to 1837 Ωm, observed across a lateral distance of 5 – 195 m, thereby categorized as lateritic subsoil.

The geoelectric profile depicted in Fig. 7 illustrates the characteristics of the subsurface layers. The first horizon, located between depths of 2.5 to 5 m, comprises lateritic topsoil intercalated with sandstones. This layer exhibits a thickness of 2.5 m and demonstrates resistivity values ranging from 1546 to 2824 Ωm. Adjacent to this, the second layer, suspected to consist primarily of sandstones, extends from 5 to 24.9 m depth, with resistivity values ranging from 2219 to 2824 Ωm. Beyond this depth, the resistivity diminishes, falling within the range of 1371 to 1744 Ωm, and is identified as lateritic subsoil, with lateral distribution spanning from 5 to 195 m.

At 2.5 – 5 m depth, resistivity within the study area exhibits a range from 767 – 1722 Ωm, indicative of lateritic topsoil, with a lateral spread covering 5 – 195 m. Subsequently, from 5 – 39.6 m depth and extending laterally from 5 – 170 m, resistivity values shift to a range of 2580 – 3865 Ωm, suggestive of sandstones. At a lateral distance spanning 175 – 195 m and within the depth range of 5 – 39.6 m, resistivity is observed to vary between 341 and 1722 Ωm, suggesting the presence of lateritic subsoil.

At a depth range of 2.5 – 18.5 m and lateral distances spanning from 5 – 105 m, as observed in Fig. 9, the resistivity values range from 1659 – 2836 Ωm, suggesting the presence of lateritic sand with sandstone intercalations. Beyond this depth range, between lateral distances of 105 – 195 m and depths of 2.5 – 39.6 m, the resistivity exhibits fluctuations between 1870 and 3838 Ωm, indicating the probable presence of sandstone. The final layer, occurring at lateral distances of 5 – 110 m and depths of 18.5 – 31.9 m, characterized by resistivity values ranging from 1659 - 2108 Ωm, is indicative of lateritic subsoil.

In the geoelectric profile represented in Fig. 10, we observe the first layer comprising lateritic topsoil with sandstone intercalations, extending 2.5 meters in thickness from a depth of 2.5 to 5 meters beneath the surface. The resistivity values within this layer range from 1504 to 2651

Ωm, spanning a lateral distance of 5 – 195 m. Moving deeper, the second horizon manifests between 5 and 20m depth, exhibiting resistivity values ranging from 2651 to 3519 Ωm. Beyond this depth range, resistivity diminishes, ranging from 1504 to 1997 Ωm, indicating the presence of lateritic subsoil.

In Fig. 11, the first layer, lateritic topsoil with sandstone intercalations, is 2.5 m thick from 2.5 – 5 m beneath the surface. Resistivity values range from 1309 to 2787 Ωm, with a lateral distance of 5 to 195 m. The second horizon occurs at 5 – 25 m depth, with resistivity values ranging from 2396 to 3241 Ωm. Beyond 25 m depth, resistivity ranges from 1309 – 1771 Ωm, noted at lateral distances of 5 – 195 m, classified as lateritic subsoil.

The first layer observed, lateritic topsoil, exhibits a thickness of 2.5 m from depths of 2.5 – 5 m beneath the surface, displaying resistivity values ranging from 1577 to 1941 Ωm. This layer extends laterally from 5 – 195 m. The subsequent subsoil stratum is encountered at depths ranging from 5 - 24.9 m, extending laterally from 5 – 195 m, with resistivity values ranging from 2154 to 2941 Ωm. As depth progresses beyond 31.9 – 39.6 m, the resistivity falls within the range of 1650 – 2154 Ωm, classifying it as lateritic subsoil (Fig. 12).

At a depth range of 2.5 – 5 m and lateral spread of 5 – 195 m (Fig. 13), resistivity values range from 1837 – 3113 Ωm, indicative of lateritic topsoil with sandstone intercalations. At 5 – 24.9 m depth and lateral distance of 5 – 195 m, resistivity falls between 3113 and 3711 Ωm, symptomatic of sandstones. At lateral distances of 5 – 195 m and a depth range of 25 – 39.6 m, resistivity ranges from 1540 to 2611 Ωm, suspected to be lateritic subsoil.

The resistivity profiling conducted in the study area reveals a diverse subsurface lithological composition. The delineation of lateritic topsoil, dry laterite, sandstones, and lateritic subsoil across various depth intervals provides valuable insights into the geological structure. The lateral extent and resistivity values of each layer indicate significant variability, reflecting the complex nature of the subsurface. For instance, the presence of lateritic topsoil with sandstone intercalations suggests a transition zone between different geological formations. The distinct resistivity ranges observed for each lithological unit further emphasize the heterogeneity of the subsurface materials. These findings have implications for various applications, including groundwater exploration, engineering projects, and land management.

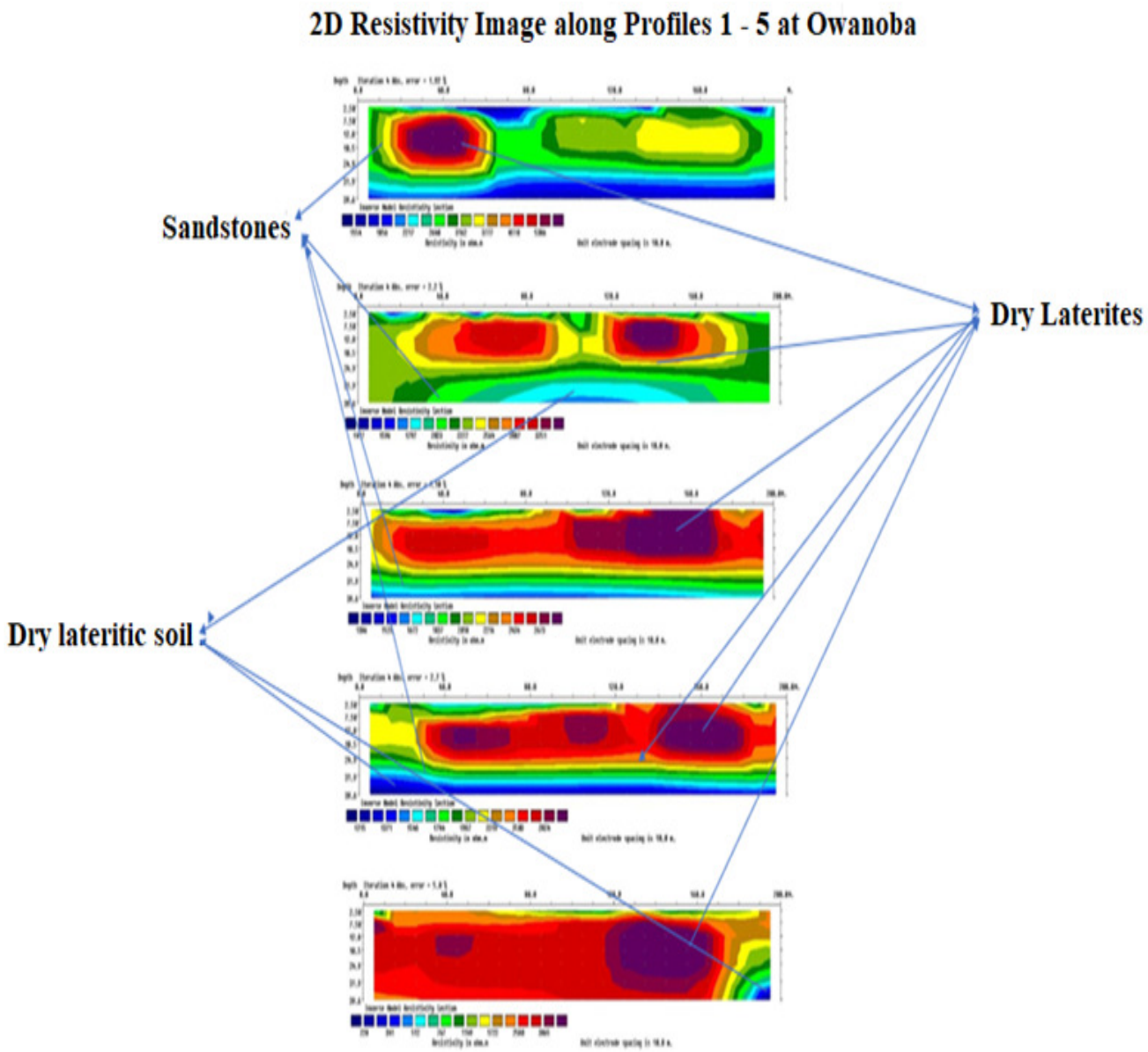

Fig. 14: Traverse 1 – 5 at Owanoba Community

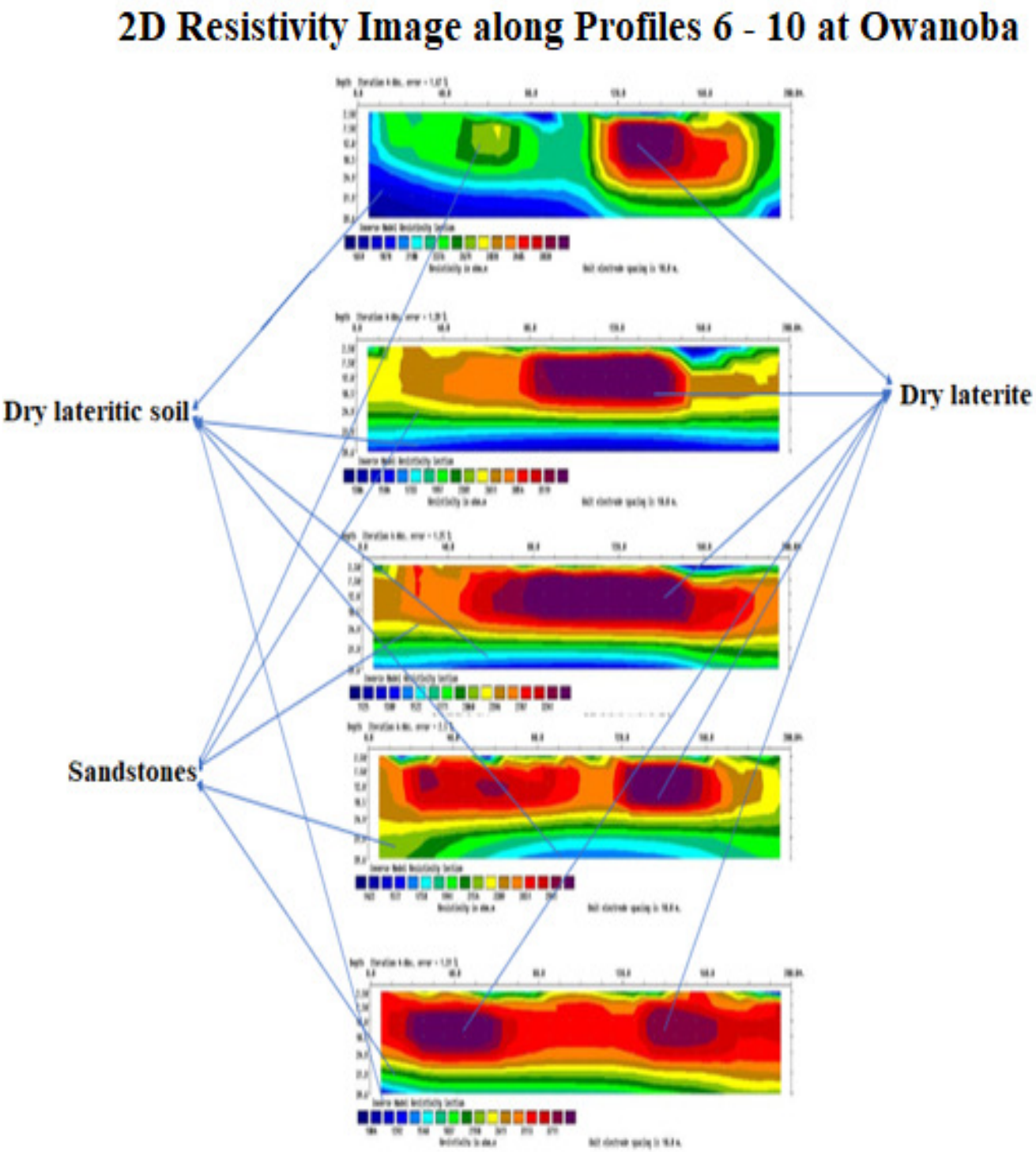

Fig. 15: Traverse 6 – 10 at Owanoba Community

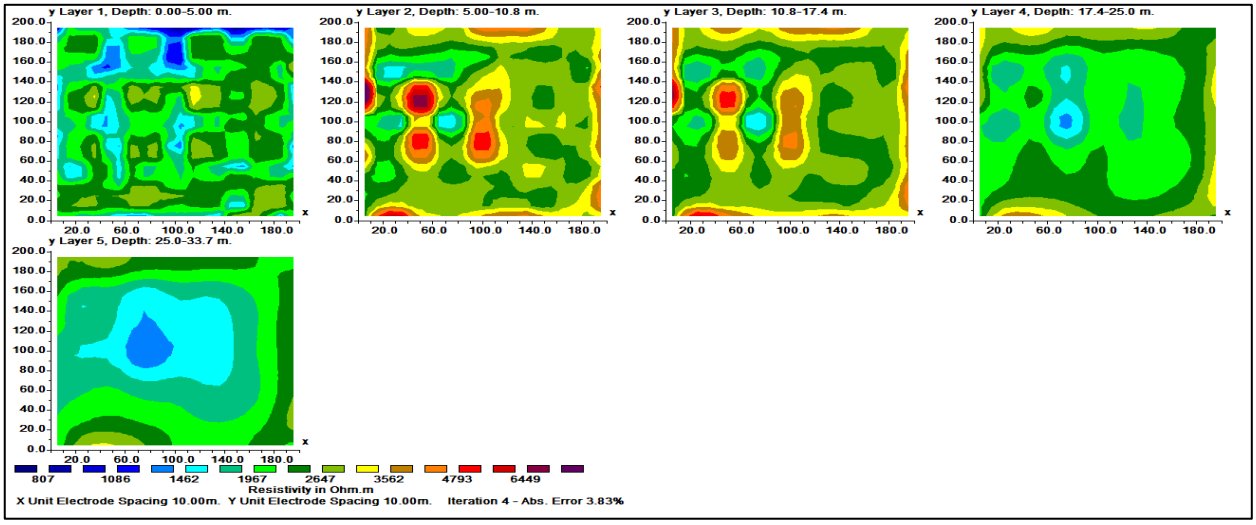

Fig. 16: Horizontal depth slices at Owanoba

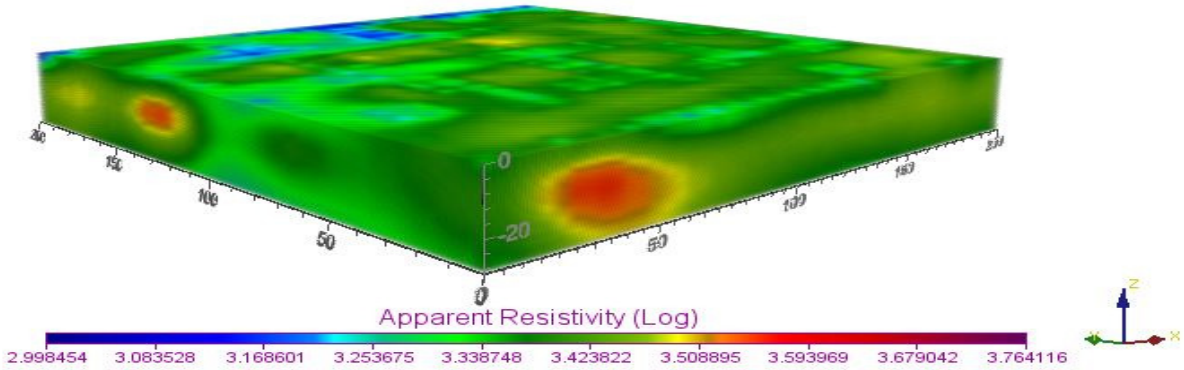

Fig. 17: 3D electrical resistivity pseudo-section along Owanoba

The volume rendering probed to a depth of 29m. The posterior view (Figure 17) of the block has a low resistivity value of about 341 Ωm. The image also showed that within the lateral view, there are pockets of relatively high-resistivity subsoil materials with maximum resistivity value of about 5,386 Ωm. These pockets of material extend from the surface to a depth of 29 m in places within the region. The result showed that the Owanoba study area is made up of resistive materials such as dry lateritic sand (341 – 2,277 Ωm), sandstones (1856 – 3865 Ωm), and wet and dry laterite (767 – 5386 Ωm).

Correlation Between Borehole Lithology in Owanoba

The lithological log for Owanoba, depicted in Figure 18, reveals details of a borehole drilled to approximately 98 meters. The log indicates that the subsurface in this location is predominantly comprised of sand, exhibiting variations in grain sizes and compactness. The uppermost layer, akin to topsoil, consists of fine to medium-grain sand and laterite, extending from the surface to around 7.5 meters. Beneath it lies a layer of coarse, dry laterite, spanning depths from about 5 meters to as far as 27 meters. Below the coarse, dry sand layer, there is a presence of medium-coarse sand material, occurring within the depth range of 25 to 40 meters.

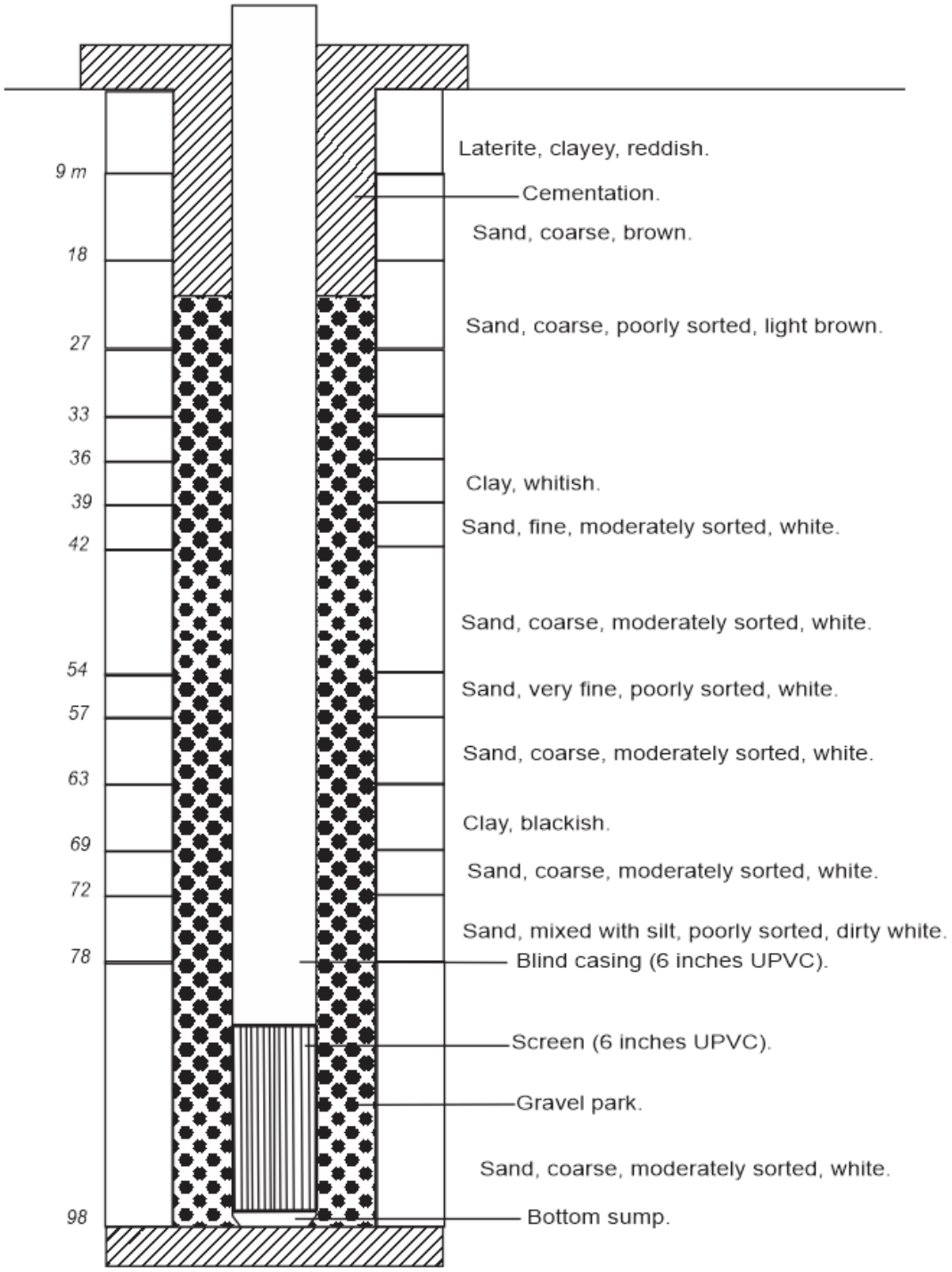

Fig. 18: Lithology logs of Owanoba
(Source: Benin Owena River Basin Development Authority)

Resistivity Lithology of the Survey Locations

A summary of resistivity lithology in Owanoba is shown in Table 1

Table 1: Resistivity Lithology of the Survey in Owanoba

Depth (m) (in range)	Resistivity (Ωm) (in range)	Lithology	Occurrence
0 – 5	807 - 1462		Lateritic topsoil
5 – 20	1462 - 4793		Dry lateritic subsoil
20 – 40	1462 - 2647		Sandstones

The resistivity lithology analysis of Owanoba revealed the existence of three geoelectric subsurface to a considerable depth of 40 meters: lateritic topsoil (807 - 1462 Ωm), sandstones with shale intercalations (1462 - 4793 Ωm), and lateritic subsurface (1462 - 2647 Ωm) in Owanoba.

The investigation carried out in our study area by Iduseri and Alile (2021) revealed a range of resistivity values for distinct lithologies, including topsoil, dry sand, partially saturated sand, and saturated sand, consistent with our findings. However, our findings showed slight variations in the vertical and lateral extents of formations such as lateritic topsoil, dry laterite, sandstones, and lateritic subsoil.

CONCLUSION

The geophysical findings unveil crucial insights into the subsurface lithological composition of the Owanoba study area. The delineation of topsoil with varying resistivity values ranging from 1554 – 5377 Ωm across depths of 2.5 – 7.5 m highlights potential soil heterogeneity. Dry laterite, indicated by resistivity values of 3777 – 5386 Ωm within the depth range of 7.5 – 24.9 m, suggests the presence of weathered material with implications for construction and land use planning. Additionally, the suspected sandstone substratum, characterized by resistivity values of 1856 to 3741 Ωm between depths of 2.5 – 20 m, underscores the geological diversity of the area. The observed variations in lateritic subsoil resistivity, ranging from 1554 to 2217 Ωm at depths of 31.9 – 39.6 m, further delineate the lithological complexity.

The geoelectric layers depicted in Figures 5, 6, and 7 provide detailed insights into the lateral distribution and resistivity characteristics of lateritic topsoil, sandstone layers, and lateritic subsoil. These findings aid in understanding the spatial variability of lithological units, crucial for groundwater exploration, engineering applications, and land management practices. Furthermore, the 3D technique applied in Figure 17 enables a comprehensive visualization of resistivity variations, revealing high-resistivity pockets and areas with low-resistivity values. Such detailed information is invaluable for geological modelling, hydrogeological studies, and environmental assessments in the region.

The integration of borehole log data with the field results was to enhance the

accuracy and reliability of the interpretations as borehole logs play crucial role in complementing and validating findings, ultimately improving the understanding of subsurface lithological complexities.

REFERENCES

Alile, O. M., Ujuanbi, O. and Evbuomwan, I. A. (2011). Geoelectric investigation of groundwater in Obaretin – Iyanomon locality, Edo state, Nigeria. *Journal of Geology and Mining Research,* 3(1): 13 – 20.

Avenbuan, N., Alile, O. M and Iduseri, O. M. (2020a). Two-Dimensional Electrical Resistivity Investigation of Plants Roots and its Implication in University of Benin Engineering Field, Ugbowo, Edo State, Nigeria. *J. Appl. Sci. Environ. Manage*., 24(11): 1867-1871. DOI: 10.4314/jasem.v24i11.4).

Avenbuan, N., Alile, O. M. and Iduseri, O. M. (2020b). A Comparative Study of Subsurface Earth Classification Between Two Dimensional and Three Dimensional Geoelectrical Imaging in University of Benin Teaching Hospital, Benin City, Nigeria. *Nigerian Research Journal of Engineering and Environmental Sciences*, 5(2): 591-601. www.rjees.com).

Gao, C., Shirota, J., Kelly, R. I., Brunton, F. R. and Van Haaften, S. (2006). Bedrock Topography and Overburden Thickness Mapping, Southern Ontario; *Ontario Geological Survey*, Miscellaneous Release—Data 207. DOI:10.13140/RG.2.1.3347.0965

Griffiths, D. H. and Barker, R. D. (1993). Two-dimensional resistivity imaging and modeling in areas of complex geology. *Journal of Applied Geophysics,* 29: 211–226. https://doi.org/10.1016/0926-9851(93)90005-J.

Iduseri, O. M. and Alile. O. M. (2021). 2D and 3D Electrical Resistivity Imaging (ERI) for Erosion Vulnerability and Subsurface Characterization for Engineering Constructions and Groundwater Potential in Owanoba and Obaretin Areas of Edo State, South-South Nigeria. *The Pacific Journal of Science and Technology*, 22(1). May 2021 (Spring)

Loke, M. and Barker, R.D. (1996). Rapid least-squares inversion of apparent resistivity pseudo sections by a quasi-Newton method. *Geophysics Prospect*, 44:131–152. ISSN: 1365-2478, 0016-8025

Loke, M. H., Chambers, J. E., Rucker, D. F., Kuras, O. and Wilkinson, P. B. (2013). Recent developments in the direct-current geoelectrical imaging method. *Journal of Applied Geophysics*, 95: 135-156. http://dx.doi.org/10.1016/j.jappgeo.2013.02.017

Rhodes, C. J. (2012). Feeding and healing the world: through regenerative agriculture and permaculture. *Sci. Prog*., 95(Pt 4): 345–446. doi: 10.3184/003685012X13504990668392.

Telford, W. M., Telford, W. M., Geldart, L. P., Sheriff, R. E. and Sheriff, R. E. (1990). Applied geophysics. Cambridge university press. ISBN-13: 978-0521339384.